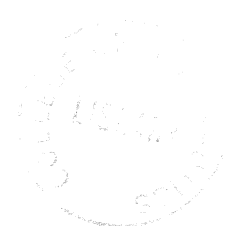




ST. M. R 33444

MINISTRY OF AVIATION

AERONAUTICAL RESEARCH COUNCIL
REPORTS AND MEMORANDA



Wind-Tunnel Experiments on the Flow over Rectangular Cavities at Subsonic and Transonic Speeds

By J. E. ROSSITER

LONDON: HER MAJESTY'S STATIONERY OFFICE

1966

PRICE 13s. 6d. NET

R 33444

Wind-Tunnel Experiments on the Flow over Rectangular Cavities at Subsonic and Transonic Speeds

By J. E. ROSSITER

COMMUNICATED BY THE DEPUTY CONTROLLER AIRCRAFT (RESEARCH AND DEVELOPMENT),
MINISTRY OF AVIATION

*Reports and Memoranda No. 3438**
October, 1964

Summary.

Measurements have been made of the time average and unsteady pressures acting on the roof and behind a series of rectangular cavities set in the roof of the 2 ft \times 1½ ft transonic tunnel.

It was found that the unsteady pressures contain both random and periodic components. The random component predominates in the shallower cavities (length/depth ratio $>$ 4) and is most intense near the rear wall. The periodic component predominates in the deeper cavities (length/depth ratio $<$ 4) and may form standing wave patterns. It is suggested that the periodic component is due to an acoustic resonance within the cavity excited by a phenomenon similar to that causing edge-tones. It may be suppressed by fixing a small spoiler at the front of the cavity.

LIST OF CONTENTS

Section

1. Introduction
2. Test Details
3. The Mean Flow over Cavities
4. The Unsteady Pressure Field
 - 4.1 Presentation of results
 - 4.2 General nature of the unsteady pressure field
 - 4.3 Random pressure fluctuations
 - 4.4 Periodic pressure fluctuations
 - 4.4.1 Frequency of periodic pressure fluctuations
 - 4.4.2 Amplitude distribution of periodic pressure fluctuations
 - 4.4.3 Shadowgraphs
 - 4.5 Effect of changing the width and length of the cavity
 - 4.6 Suppression of periodic pressure fluctuations
5. Discussion on the Periodic Pressure Fluctuations
6. Conclusions

* Replaces R.A.E. Tech. Report No. 64037—A.R.C. 26 621.



LIST OF CONTENTS—*continued*

Section

Symbols

References

Illustrations—Figs. 1 to 22

Detachable Abstract Cards

1. *Introduction.*

The flow of air over an open cavity formed in the surface of an aeroplane is usually unsteady, and large fluctuations may occur in the pressure acting on the walls of the cavity and on surrounding surfaces. These fluctuations in air pressure can excite vibration of the local structure, and, if the cavity is a large one such as a bomb bay, of the main flexural modes of the aeroplane. Before the magnitude of the vibration can be estimated it is necessary to know the nature of the unsteady pressure field.

A low-speed wind-tunnel investigation¹ into the unsteady pressures in bomb bays made during 1952 and 1953 at the Royal Aircraft Establishment, Farnborough, showed that for shallow and moderately deep bomb bays (length/depth ratio > 5) the unsteady pressure field is random in character for airspeeds up to 300 ft/s. It was found that if the measured pressure fluctuations were analysed in terms of their frequency content, then the spectrum covered a broad band of frequencies (about 8 octaves). Further, for a given bay geometry, the magnitude of the unsteady pressures was proportional to free-stream kinetic pressure, and the frequency scale was proportional to free-stream velocity and inversely proportional to the length of the bay.

While these investigations were being made at R.A.E., similar investigations² made in America on a B.47 aircraft at rather higher speeds, showed that in addition to random pressure fluctuations, strong periodic pressure fluctuations may occur in the flow over bomb bays. The nature of these periodic pressure fluctuations has been investigated by Krishnamurty³ and by Plumblee *et al*⁴. Krishnamurty, experimenting on very small (depth = 0.1 inches) two-dimensional cavities, found that the periodic pressure fluctuations are accompanied by strong acoustic radiation from the cavity, and that their frequency increases with airspeed and decreases as the cavity length is increased. Plumblee *et al* calculate the acoustic resonant response of a cavity placed in an airstream and compare the answers with experiments on cavities set in a body of revolution. They conclude that the periodic pressure fluctuations in cavities are due to an acoustic resonance excited by the unsteadiness in the turbulent boundary layer approaching the cavity. However this hypothesis is untenable since, as Krishnamurty found, the periodic pressure fluctuations are present when the boundary layer is laminar. Nevertheless it would appear that acoustic resonance does play an important part in determining the frequency and magnitude of the pressure fluctuations but the forcing function is a property of the flow over the cavity rather than of the boundary layer approaching it.

In order to establish under what conditions periodic and/or random pressure fluctuations occur, wind-tunnel experiments were made during 1962 on a series of rectangular cavities set in the roof of the 2 ft \times 1½ ft transonic tunnel. The results of this investigation were used as the basis for an unpublished paper⁵ presented to the Structures and Materials Panel of AGARD in July, 1962. However some of the experimental results appear to be of sufficient interest to warrant this more formal presentation.

2. Test Details.

The tests were made on a rectangular cavity set in the roof of the 2 ft \times 1½ ft transonic tunnel. The cavity had a length of 8 inches, a width of 4 inches and the depth could be varied from 0.8 to 8 inches. Packing blocks could be used to reduce the width of the cavity to 2 inches and these were in position for most of the test. Small differential capacity-type pressure transducers⁶ were used to measure the unsteady pressures acting at 9 positions along the roof of the cavity and 3 positions along the roof of the tunnel behind the cavity as shown in Fig. 1. The transducers were mounted between rubber pads and held by clamping plates so that the orifice on one side of a transducer was flush with the surface. The orifice on the other side of a transducer was connected through a long length (about 50 ft) of small-bore tubing to tunnel static pressure. The transducers were calibrated before each test period by applying a known steady pressure to each transducer in turn and observing the outputs from the transducer amplifiers on a d.c. voltmeter. Variations in the calibration factors throughout the tests were less than $\pm 3\%$. The frequency response of the transducers and their amplifiers were checked before the test began, by subjecting the transducers to a pressure step in a shock tube. The response was found to be flat up to 5 Kc/s.

During the test the outputs from the transducer amplifiers were measured on a Dawes 'True r.m.s.' meter (Type 612A) and the outputs from selected amplifiers were recorded on an Ampex Type 306-2 tape recorder for subsequent analysis using a Muirhead-Pamatrada Type D489 frequency analyser with a bandwidth ratio of 15.5%. The recording and analysing system is described fully in Ref. 1. Sufficient measurements were made to define the distribution of the unsteady pressure in terms of r.m.s. values for 6 cavity depths over a Mach number range from 0.4 to 1.2 with Reynolds number held constant at 2.2 million per foot. Frequency spectra were in general measured for only one point in the cavity ($x/L = 0.9$) but more extensive measurements were made on cavities with length/depth ratios of 2 and 10. In addition the effect of Reynolds number was investigated on a cavity with a length/depth ratio of 4 as was the effect of altering the length and width while keeping the length/depth ratio fixed.

In addition to the unsteady pressure measurement, time average pressures were measured by conventional manometers connected to pressure tapings in the roof of the cavity and in the tunnel roof behind the cavity.

The total head pressure distribution in the boundary layer on the tunnel roof was measured in the absence of the cavity (*see* Fig. 2). The boundary-layer thickness was 0.65 inches at subsonic speeds and 0.55 inches at $M = 1.2$ and the corresponding displacement thickness, δ^* , was 0.105 inches and appeared to be independent of Mach number.

Amplitude spectra (*see* Section 4.1) of the pressure fluctuations measured on the tunnel roof in the absence of the cavity are shown in Fig. 3. Also shown in this figure is the amplitude spectrum of the electronic noise from the transducer amplifiers. It will be seen that the tunnel 'noise' is small compared with the pressure fluctuations in the cavity (*see* Fig. 7) for $n < 2$.

3. The Mean Flow over Cavities.

Before presenting the results of the unsteady pressure measurements, it will be useful to discuss briefly the nature of the time average flow over cavities. It must be remembered that the real flow is highly unsteady and that the flow patterns discussed in this section do not necessarily correspond to features which could be observed in the flow at any instant of time.

Considering first the case of two-dimensional cavities, Roshko⁷ has shown that the type of mean flow pattern depends critically on the length/depth ratio of the cavity. For very shallow cavities, the flow over the front and rear walls may be considered independently as the flow down and up a step respectively. The airflow will separate from the front edge and reattach at some point along the roof of the cavity. The pressure in the separated region will be somewhat lower than the free-stream pressure, because of the speeding up of the external stream as it enters the cavity but will rise again at the attachment point. As the airflow approaches the rear wall, it will be retarded and the pressure will rise until a point is reached at which the boundary layer separates again to form the boundary of a high-pressure separated region ahead of the rear wall. The boundary layer may reattach somewhat downstream of the cavity. If the length/depth ratio of the cavity is decreased, the attachment and separation point on its roof will move closer together until a reverse flow develops between the high-pressure region ahead of the rear wall and the low-pressure region behind the front wall. A large captive eddy will then form within the cavity.

The same basic type of flow patterns occur on the centreline of three-dimensional cavities even when the width is much smaller than the length as has been shown by Fail *et al*⁸. There is, however, an important difference between the flow associated with two- and three-dimensional cavities. In the two-dimensional case, the eddies in the corners of a shallow cavity and the single captive eddy in a deep cavity will be separated from the external stream by dividing streamlines. In the three-dimensional case there is no such restriction and air can be drawn continuously into the eddies from the external stream and escape in a trailing vortex system shed from the cavity. Thus although the flow on the centreline of a three-dimensional cavity may be somewhat similar to that in a two-dimensional cavity, the flow near the sides and downstream will be quite different.

The distribution of the mean pressure in and behind the cavities is shown in Figs. 4 and 5. Some results of an investigation by Roshko⁷ have been included in Fig. 4. While these results are not directly comparable to those from the present test because of the smaller length/width ratio and the relatively thicker boundary layer approaching the cavity, they have been included in order to show the type of pressure distribution occurring in very shallow cavities. For the shallow cavities the pressure rises associated with flow attachment and separation on the roof of the cavities may be seen. Immediately behind the cavity the pressure reaches a very low value. At a length/depth ratio of 8, the two pressure rises have merged and at a length/depth ratio of 6, the pressure is almost constant along the roof of the cavity indicating that the two separations have combined. For the deeper cavities there is a decrease in the pressure on the roof associated with the high airspeeds at the periphery of the captive eddy.

As Mach number is increased, the flow attachment point on the roof of the shallower cavities moves downstream (see Nash's⁹ experiments on the flow over steps) so that the cavities become effectively deeper. As a result the pressure distributions (Fig. 5) for the shallower cavities show a large variation with Mach number whereas the pressure distributions in the deeper cavities are comparatively independent of Mach number.

4. *The Unsteady Pressure Field.*

4.1. *Presentation of Results.*

The unsteady pressures are described by their r.m.s. values and by their amplitude spectra. The root mean square of the unsteady pressures have been made non-dimensional by dividing them by tunnel kinetic pressure q , to give $\Delta C_{p\text{ rms}}$.

In the frequency spectra, a non-dimensional frequency parameter n has been introduced such that

$$n = f \frac{L}{U} \quad (1)$$

where f is measured frequency (c/s)

L is a representative length (the cavity length has been used) (ft)

U is tunnel velocity (ft/s)

The ordinate of an amplitude spectrum is $p_\epsilon/q\sqrt{\epsilon}$ where

p_ϵ is the r.m.s. of the pressure fluctuations corresponding to the voltage passed by the frequency analyser

and ϵ is the bandwidth ratio of the frequency analyser ($= 0.155$).

If the pressure fluctuations are random in character, so that the ordinate of the spectrum varies slowly with frequency, then $p_\epsilon/q\sqrt{\epsilon}$ is independent of ϵ and can be related to the power spectral density $F(n)$ defined by

$$(\Delta C_{p \text{ rms}})^2 = \int_0^\infty F(n)dn, \quad (2)$$

i.e. $F(n)dn$ is the contribution to $(\Delta C_{p \text{ rms}})^2$ in the frequency band n to $(n + dn)$, so that

$$\left(\frac{p_\epsilon}{q}\right)^2 = \int_{n(1-\epsilon/2)}^{n(1+\epsilon/2)} F(n)dn \doteq F(n)n\epsilon$$

since $F(n)$ is a slowly varying function and ϵ is small. Hence

$$\frac{p_\epsilon}{q\sqrt{\epsilon}} = \sqrt{\{nF(n)\}}. \quad (3)$$

If a peak occurs in a spectrum its shape will be determined by the analyser response. A discrete frequency will appear in the spectrum as a peak having the same shape as the analyser response curve and the r.m.s. of the pressure fluctuations at the discrete frequency may be determined by

$$[\Delta C_{p \text{ rms}^2}]_P = \epsilon \left\{ \left(\frac{p_\epsilon}{q\sqrt{\epsilon}}\right)_P^2 - \left(\frac{p_\epsilon}{q\sqrt{\epsilon}}\right)_R^2 \right\} \quad (4)$$

where the suffix P refers to the peak

and R to the general level around the peak.

4.2. General Nature of the Unsteady Pressure Field.

Time histories of the pressure fluctuations at a point near the rear of the cavities for $M = 0.4$ are shown in Fig. 6. In the deep cavities, $L/D = 1$ and 2 , the pressure fluctuations are mainly periodic but as the cavity depth is decreased the fluctuations become random in character. This is demonstrated more clearly by the amplitude spectra shown in Fig. 7. For the very shallow cavity ($L/D = 10$) at $M = 0.4$, the spectrum is smooth and covers a broad band of frequencies showing that the pressure fluctuations are random in character. As the depth of the cavity is increased, peaks occur in the spectra indicating that periodic pressure fluctuations are superposed upon the random level. For the deeper cavities ($L/D = 1$ and 2) the periodic component predominates and the random component becomes quite small. The effect of increasing Mach number is to increase the magnitude of the periodic component.

It should perhaps be noted that the depth of the shallower cavities was of the same order as the thickness of the boundary layer approaching the cavity and, as will be shown later, the ratio of boundary-layer thickness to cavity depth is an important parameter in determining the magnitude of the periodic pressure fluctuations. It might therefore be argued that the absence of periodic pressure fluctuations in the shallow cavities is due to the relatively thick boundary layer. However Owen's¹ experiments, where the boundary-layer thickness was small compared with the cavity depth ($\delta^*/L = 0.0018$) show that periodic pressure fluctuations do not occur in shallow cavities, at least at low speed.

It should be appreciated that the term 'periodic' is being used rather loosely. In the deeper cavities the fluctuations are confined to a very narrow frequency band (less than that of the analyser) and for practical purposes it is probably justifiable to regard them as occurring at a discrete frequency. In the shallower cavities, on the other hand, the peaks are somewhat broader and represent a narrow band of preferred frequencies rather than a single discrete frequency.

4.3. *Random Pressure Fluctuations.*

The random component of the pressure fluctuations predominates in the shallower cavities. Fig. 8 shows the distribution of the unsteady pressures in terms of their r.m.s. values for cavities with length/depth ratios of 6, 8 and 10. The pressure fluctuations are most intense near the rear wall of the cavity and decrease in magnitude with distance both forward along the roof of the cavity and rearward along the surface behind the cavity. However for the cavity with a length/depth ratio of 10 at $M = 0.5$ there is a local maximum in the intensity at about the position where the flow reattaches to the roof. The high level of the fluctuations immediately behind the cavities may possibly be associated with an intermittent venting of the high-pressure separation to the low-pressure region immediately behind the cavity. In general increasing Mach number decreases the intensity of the pressure fluctuations. The effect is small along the roof but behind the cavity the pressure fluctuations for the two shallower cavities are approximately halved as speed is increased from $M = 0.5$ to 1.2. The increase in the r.m.s. of the pressure fluctuations for the cavity with $L/D = 6$ as Mach number is increased is due to the growth in the periodic component.

Amplitude spectra for 3 positions along the roof and one behind the cavity with a length/depth ratio of 10 are shown in Fig. 9. For $x/L = 0.4$, i.e. near the reattachment point the spectrum is smooth and hump shaped with a maximum at about $n = 1$. At $x/L = 0.6$ the spectrum is similar to that for $x/L = 0.4$ but is moved up the frequency scale. At $x/L = 0.9$ the spectrum again covers the same frequency range as at $x/L = 0.4$ but has almost exactly twice the magnitude. Behind the cavity, at $x/L = 1.05$ the spectrum shows a large increase in the fluctuations at the higher end of the frequency range.

More detailed measurements of the unsteady pressures in a shallow cavity are given in Ref. 10 which describes wind tunnel tests made on the bomb bay in a model of the *Canberra* aircraft.

4.4. *Periodic Pressure Fluctuations.*

4.4.1. *Frequency of periodic pressure fluctuations.*—For the deeper cavities, there is usually one peak in the amplitude spectra which is very much larger than the others, whereas for the shallower cavities there are usually two or more peaks of almost equal magnitude.

The frequencies at which the peaks occur in the spectra for the cavities with length/depth ratios of 1 and 2 are shown in Fig. 10. The frequencies of the larger peaks (the dominant frequencies) are

shown by filled in symbols and it will be seen that, as speed is increased, the dominant frequency ‘jumps’ from one value to another in what appears to be an arbitrary manner. These jumps were usually quite abrupt but for the cavity with a length/depth ratio of 2 there was a small Mach number range around 0.7 where no one frequency was dominant. In addition to the dominant frequencies, two other sets of frequencies may be distinguished from the amplitude spectra. Firstly, there are peaks which are at integral multiples of the dominant frequency (*see* for example Fig. 7, $L/D = 1$, $M = 0.9$). These harmonics have not been included in Fig. 10 since they probably represent distortions of the pressure fluctuations from a pure sine wave rather than a separate physical phenomenon. Secondly, there are peaks in the spectra which occur at frequencies which are not simple multiples of the dominant frequency, and these have been included in Fig. 10. Because of the wide bandwidth of the analyser, it was not always possible to distinguish, with certainty, between these secondary frequencies and harmonics of the fundamental. When such uncertainty existed, the points have been omitted from Fig. 10. It will be seen that these secondary frequencies lie on a family of curves which also include the dominant frequencies and that the jumps in the dominant frequency are from one curve to another. At a given Mach number, the frequency at which the peaks occur lie in a sequence of the form $(m - \gamma)$ where $m = 1, 2, 3 \dots$ and $\gamma = 0.25$ for these two cavities. This sequence of frequencies is the same as that found by Brown¹¹ in his classic experiments on the ‘edge-tone’ which occurs when a wedge is placed in a laminar jet issuing from a narrow slit. Brown referred to the frequency ranges between jumps as stages and, since it seems probably that the two phenomena are related, it is convenient to use the same nomenclature, so that frequencies corresponding to $m = 1, 2, 3$, etc. will be called stages 1, 2, 3, etc.

It was found that the frequencies measured could be represented by the empirical equation

$$f = \frac{U}{L} \frac{(m - \gamma)}{\left(\frac{1}{K} + M\right)} \quad (8)$$

where K is a constant. The physical implications of this equation are discussed in Section 5.

In the shallower cavities (length/depth ratios from 4 to 10) there are generally two or more peaks of similar magnitude in the amplitude spectra. The frequencies at which the peaks occur are plotted against Mach number in Fig. 11. For the cavities of medium depth, the ratios of the frequencies occurring at any Mach number are almost the same as for the deep cavities but in the shallower cavities the ratios are rather different. Values of γ , averaged over the speed range are given in the table below.

L/D	γ
4	0.25
6	0.38
8	0.54
10	0.58

The family of curves given by equation (8) for $\gamma = 0.25$ and $K = 0.57$ (derived from $L/D = 4$) are shown in Fig. 11 and it will be seen that the experimental points for all these cavities lie tolerably close to the curves despite the differences in the values of γ .

4.4.2. *Amplitude distribution of periodic pressure fluctuations.*—The periodic pressure fluctuations in the deep cavities were so regular that it was possible to measure the change of phase along the roof of the cavity. For the cavity with a length/depth ratio of 2, the outputs from the transducers were passed in turn, through a filter with a bandwidth ratio of 5% tuned to the dominant frequency. The r.m.s. of the filtered outputs and the phase angle relative to the transducer at $x/L = 0.1$ were measured using a Muirhead Phasemeter Type D-729-B. The results are given in Fig. 12. It will be seen that three distinct phase patterns can exist, depending on the Mach number. For $M = 0.4$ and 0.7 there is a small phase change along most of the length of the cavity. For $M = 0.35, 0.5$ and 1.2 , there is a phase change of approximately π halfway along the roof and for $M = 0.68$ there are two phase changes of approximately π along the roof of the cavity. It is convenient to refer to these distributions as mode shapes I, II and III respectively. The phase changes occurring in mode shapes II and III show that standing wave patterns exist within the cavity with pressure nodes where the phase changes occur. The existence of these nodes is confirmed by the filtered r.m.s. of the pressure. The phase changes occurring in mode shape I show that periodic disturbances (possibly pressure waves) are travelling upstream from the back to the front of the bay. At $M = 0.7$ there was no distinct dominant frequency and the phase measurements were made for the frequency at which the pressure fluctuations were strongest.

Detailed measurements were not made of the mode shapes for the cavity with a length/depth ratio of unity, but oscilloscope observations during the tests enabled the mode shapes to be determined, and these have been confirmed by examining the distribution of the r.m.s. of the pressure fluctuations (*see* Fig. 13).

The mode shapes have been indicated in Fig. 10 for the cavities with $L/D = 1$ and 2 and it will be seen that they do not correspond to the stages already discussed but rather to particular values of frequency.

The magnitudes of the periodic component of the unsteady pressures in the shallower cavities have been deduced using equation (4) for a point near the rear of the cavities and are given in Fig. 14. It is difficult to separate the periodic from the random component sufficiently to see the type of wave pattern in these shallow cavities but the distribution of the r.m.s. of the pressure fluctuations for the cavity with $L/D = 6$ (Fig. 8a) and $L/D = 4$ (Fig. 18a) suggest that mode shape III may exist at the higher Mach numbers.

4.4.3. *Shadowgraphs.*—Shadowgraphs of the external flow over the cavity with a length/depth ratio of 2 at $M = 1.2$ are shown in Fig. 16. These photographs were taken at random time intervals using a flash tube with a duration of a few microseconds. A high-speed cine film of the same configuration has enabled the photographs to be put in a correctly timed sequence and the reconstruction of the flow patterns sketched in Fig. 17 to be made.

These photographs do not show what is happening inside the cavity, and to assist in their interpretation, shadowgraphs of the flow in a small two-dimensional cavity are shown in Fig. 15. From these it can be seen that the shear layer separating the cavity from the external stream rolls up into discrete vortices which are shed at regular time intervals from the front lip of the cavity. Only the tops of these vortices can be seen in the photographs of Fig. 16. Measuring time from an arbitrary datum, then at $t = 0$ a vortex A forms just downstream of the front edge of the cavity. The vortex grows rapidly slowing the external stream and producing the bow wave B. As the vortex moves over the cavity, three additional pressure waves C, D and E appear ($t = 0.3T$) of these E is thought

to be a breakdown shockwave in an intermittent outflow from the cavity. The existence of this outflow is indicated by the distortion of the rear edge of the cavity in the shadowgraph (Fig. 16) and more distinctly by the ‘plume’ in the second of the sequence of photographs in Fig. 15. At $t = 0.57T$ these waves have strengthened and at $t = 0.62T$, it would appear that wave D has moved relative to wave C so as to intersect it. The high-speed outflow has ceased so that wave E becomes detached from the cavity. At $t = 0.77T$ the vortex is at the rear wall of the cavity and approximately one quarter of a period later (at $t = T$ or 0) a new vortex forms at the front edge of the cavity. There are thus four distinct sets of pressure waves radiated from the cavity. Waves B and C, which appear when the vortex is formed and when it is in the vicinity of the rear wall, respectively, and wave E which is associated with an intermittent outflow from the cavity are all approximately tangential to Mach lines and are therefore initiated by disturbances which occur at points more or less fixed relative to the cavity. Wave D, however, is not initially tangential to a Mach line and could be due to a disturbance which travels from the back to front wall of the cavity. These waves constitute an acoustic radiation from the cavity. It should be remembered that the shadowgraph technique shows effectively only the compression waves and that there is no reason to assume that the radiation is impulsive rather than continuous.

4.5. *Effect of Changing the Width and Length of the Cavity.*

The effect on the unsteady pressures of increasing the width of a cavity was investigated on the cavity with a length/depth ratio of 4 by removing the packing blocks (*see* Section 2). Typical results are shown in Figs. 18 and 19. It will be seen that the change in width made little difference to the magnitude of the random component of the pressure fluctuations or to the frequencies of the periodic components, but had a large effect on the magnitude of the periodic component. At $M = 1.2$ for example, with $L/W = 4$, the dominant frequency was in stage 2 with mode shape III whereas with $L/W = 2$, the dominant frequency was in stage 1 with mode shape II.

A brief investigation into the effect of changing Reynolds number was made on the cavity with a length/depth ratio of 4 and a length/width ratio of 2. It was reasoned that there are two ways in which a change in Reynolds number could affect the unsteady pressures. Firstly, by changing the nature of the mixing in the shear layer separating the cavity from the external stream and secondly by changing the thickness of the boundary layer approaching the cavity relative to the depth of the cavity. The first of these was investigated by changing the air density. It was found that reducing the density by one half made little difference to the boundary-layer thickness and produced no measurable change in the unsteady pressure. To investigate the second effect the cavity was shortened but its length/depth and length/width ratio were kept the same. The change was achieved by inserting an additional packing block into the cavity with a length/depth ratio of 8 and a length/width ratio of 4 which halved its length. The results are shown in Figs. 18 and 19. The shapes of the amplitude spectra are similar, which justifies the use of the cavity length to form the non-dimensional frequency parameter, but there is a decrease in the magnitude of both the random and periodic components and also a change in the relative magnitude of the peaks.

4.6. *Suppression of Periodic Pressure Fluctuations.*

The large effect of changes in the thickness of the boundary layer relative to the cavity geometry, suggested that a spoiler ahead of the cavity would reduce the magnitude of these pressure fluctuations. Tests were made with the three simple spoilers shown in Fig. 20 ahead of the cavity with a

length/depth ratio of 1 and the results are shown in Fig. 21. It will be seen that even a small spoiler produces a large reduction in the magnitude of the periodic pressure fluctuations.

5. Discussion on the Periodic Pressure Fluctuations.

The evidence from this experimental investigation show that the principal characteristics of the periodic pressure fluctuations which occur in cavities are:

- (i) The pressure fluctuations may contain a number of periodic components, whose frequencies lie in a sequence $(m - \gamma)$ where $m = 1, 2, 3 \dots$ and $\gamma < 1$.
- (ii) The frequency of any component is inversely proportional to cavity length and increases with tunnel Mach number or velocity. It was not possible to vary Mach number and velocity independently in these tests, but dimensional considerations suggest that

$$f \frac{L}{U} = f(M, Re) \quad (9)$$

and following on from this, equation (8) suggests that if velocity were held constant then the frequency would decrease with increasing Mach number. Over the range of the experiments the effect of Reynolds number was small (*see* Section 4.5).

(iii) The shadowgraphs show that the pressure fluctuations are accompanied by the periodic shedding of vortices from the front lip of the cavity and by acoustic radiation from the cavity, the principal source being close to the rear lip of the cavity.

(iv) Under some conditions standing wave patterns occur in the cavity and it is not unreasonable to assume that these are due to an acoustic resonance within the cavity.

These characteristics suggest a possible physical model of the flow. It is envisaged that a phenomenon similar to that producing edge-tones and involving the periodic shedding of vortices from the front lip of the cavity and an acoustic source at the rear lip, produces a number of periodic pressure fluctuations whose frequencies lie in the sequence $(m - \gamma)$. When the frequency of one of these components is close to the natural frequency of the volume of air in the cavity, resonance occurs.

The calculation of cavity resonance has been investigated by Plumblee *et al*⁴. It is not proposed to discuss this further, other than to note that the frequencies for mode shape I (Figs. 10 and 12) in the cavity with a length/depth ratio of unity is about one half that for the cavity with a length/depth ratio of 2 suggesting that cavity depth is the important geometric parameter in this mode. The frequency corresponding to mode shape II, however, is almost the same for the two cavities, suggesting that cavity length is the important parameter in this mode.

It was noted in Section 4.4.1, that the sequence of frequencies which occur in a cavity, is similar to that found by Brown¹¹ in his experiments on edge-tones. The regular shedding of vortices found in the flow over cavities is also a feature of the edge-tone phenomenon, as is the strong acoustic radiation. It is reasonable to assume that there is some connection between the vortex shedding and the acoustic radiation. Let us further assume that the acoustic radiation initiates the vortex shedding and that the passage of the vortices over the rear lip of the cavity is responsible for the acoustic radiation. If the average speed of the vortices over the cavity is k times the free-stream speed and sound waves travel upstream in the cavity at a mean speed c , then

$$f = \frac{kU}{\lambda_v} = \frac{c}{\lambda_a} \quad (10)$$

where λ_v is the spacing of the vortices and λ_a is the wavelength of the sound waves in the cavity, and it is assumed that the frequency of the acoustic radiation is the same as the vortex shedding frequency.

The phase relationship between the two motions is not known, but it is possible to proceed by identifying the particular phase of the acoustic radiation which reaches the front lip of the cavity at the instant that a vortex is shed, and by saying that a vortex is $\gamma_v \lambda_v$ behind the rear lip when this particular phase of the acoustic radiation leaves the source at the rear lip. For generality, it will be assumed that m_v complete wavelengths of the vortex motion are involved and m_a complete wavelengths of the acoustic radiation.

At time $t = 0$, say, an identified phase of the acoustic radiation leaves the rear lip of the cavity and a vortex is $\gamma_v \lambda_v$ behind the rear lip as shown in Fig. 22a. At time $t = t'$ an identified phase of the acoustic radiation arrives at the front lip just as a vortex is shed (Fig. 22b). The vortex pattern has moved downstream a distance kUt' in this time interval so that

$$m_v \lambda_v = L + \gamma_v \lambda_v + kUt'. \quad (11)$$

In the same time interval the internal wave system has moved a distance ct' so that

$$L = m_a \lambda_a + ct'. \quad (12)$$

Eliminating t' between (11) and (12)

$$\frac{kU}{c} m_a \lambda_a + (m_v - \gamma_v) \lambda_v = kL \left(M \frac{a}{c} + \frac{1}{k} \right)$$

and substituting for λ_a and λ_v from equation (10)

$$f = \frac{U (m_a + m_v - \gamma_v)}{L \left(M \frac{a}{c} + \frac{1}{k} \right)}. \quad (13)$$

Comparing this with the empirical equation (8) it can be seen that the postulated motion is compatible with the experimental results if

$$\left. \begin{aligned} m_v + m_a &= m \\ \gamma_v &= \gamma \\ k &= K \\ a &= c. \end{aligned} \right\} \quad (14)$$

Thus the constant K in equation (8) has now been identified as the proportion of the free-stream speed at which the vortices travel over the cavity. Measurements from the shadowgraphs of Fig. 16, for the cavity with a length/depth ratio of 2, show that the vortices are travelling at an almost constant speed equal to two-thirds of the free-stream speed which is the value of K required in equation (8) to satisfy the experimental results.

The equating of the propagation speed of sound waves in the cavity with the free-stream speed of sound needs some comment. It is to be expected that the temperature in the cavity will lie somewhere between the total head and static temperatures of the free stream. However over the speed range of these experiments, the two temperatures only differ by about 20% so that the use of the free-stream temperature, rather than the correct but unknown value, to calculate the speed of sound will involve an error of less than 10%. It is further implied that the air in the cavity is comparatively stationary and hence that the captive eddy discussed in Section 3 is weak.

Although no direct evidence of the existence of these sound waves exist it is possible that wave D discussed in Section 4.4.3 results from the propagation of such sound waves through the shear layer into the free stream.

On the basis of this analysis, it seems reasonable to conclude that the periodic pressure fluctuations are initiated by an aero-acoustic phenomenon. However the details of the mechanism outlined above should be regarded as merely an attempt to give a simplified explanation of what is undoubtedly a highly complex motion. The type of motion envisaged is by no means unique, and it is of interest that the method of analysis is similar to that used by Powell¹² to explain the instability of a jet above the critical pressure ratio.

6. *Conclusions.*

(i) The unsteady pressures acting in and around a rectangular cavity in a subsonic or transonic airflow may contain both random and periodic components. In general the random component predominates in shallow cavities ($L/D > 4$) and the periodic component predominates in deep cavities ($L/D < 4$).

(ii) The random component is most intense near the rear wall of the cavity, but for very shallow cavities a local region of intense pressure fluctuations occurs where the airflow attaches to the roof of the cavity.

(iii) The periodic pressure fluctuations appear to be due to an acoustic resonance within the cavity, excited by a phenomenon similar to that causing edge-tones. The periodic pressure fluctuations may be very large; r.m.s. values up to 0.35 times the free-stream kinetic pressure have been measured.

(iv) The periodic pressure fluctuations may be suppressed by fixing a small spoiler ahead of the cavity.

SYMBOLS

a	Speed of sound at free-stream static conditions, ft/s
b	Width of spoiler
c	Mean speed of sound in cavity, ft/s
C_p	Pressure coefficient
$\Delta C_{p\text{ rms}}$	Root mean square of pressure fluctuations divided by tunnel kinetic pressure
d	Depth of spoiler, ft
D	Depth of cavity, ft
f	Frequency, c/s
$F(f)$	Power spectral density
k	Proportion of free-stream speed U at which vortices travel over cavity
K	A constant {see equation (8)}
L	Length of cavity, ft
m	} An integer
m_a	
m_v	
M	Tunnel Mach number
n	Non-dimensional frequency parameter ($= fL/U$)
p_e	Root mean square of pressure fluctuations in frequency band ϵf , lb/ft ²
q	Tunnel kinetic pressure, lb/ft ²
Re	Reynolds number
T	Periodic time, s
U	Tunnel speed, ft/s
W	Width of cavity, ft
γ	} Constants
γ_v	
ϵ	Bandwidth ratio = $\frac{\text{frequency band}}{\text{centre frequency}}$
λ_a	Wavelength of sound waves in cavity, ft
λ_r	Spacing of vortices over cavity, ft
ϕ	A phase angle, rad

A bar over a quantity indicates its time average value.

REFERENCES

- | <i>No.</i> | <i>Author(s)</i> | <i>Title, etc.</i> |
|------------|--|---|
| 1 | T. B. Owen | Techniques of pressure-fluctuation measurements employed in the R.A.E. low speed wind tunnels.
A.G.A.R.D. Report 172.
A.R.C. 20 780. March, 1958. |
| 2 | D. A. Norton | Investigation of B47 bomb bay buffet.
Boeing Airplane Co. Document No. D12675. May, 1952. |
| 3 | K. Krishnamurty | Acoustic radiation from two-dimensional rectangular cutouts in aerodynamic surfaces.
N.A.C.A. Tech. Note 3487. August, 1955. |
| 4 | H. E. Plumlee, J. S. Gibson and
L. W. Lassiter. | A theoretical and experimental investigation of the acoustic response of cavities in an aerodynamic flow.
WADD TR-61-75, March, 1962.
A.R.C. 24 652. March, 1963. |
| 5 | J. E. Rossiter | Unpublished M.o.A. Report. April, 1962. |
| 6 | W. R. Macdonald and P. W. Cole | A sub-miniature differential pressure transducer for use in wind tunnel models.
R.A.E. Tech. Note Instn. 169. January, 1961. |
| 7 | A. Roshko | Some measurements of flow in a rectangular cutout.
N.A.C.A. Tech. Note 3488. August, 1955. |
| 8 | R. Fail, T. B. Owen and R. C. W.
Eyre. | Low speed tunnel tests on the flow in bomb bays and its effect on drag and vibration.
A.R.C. 17 412. May, 1954. |
| 9 | J. F. Nash, V. G. Quincey and
J. Callinan. | Experiments on two dimensional base flow at subsonic and transonic speeds.
A.R.C. R. & M. 3427. January, 1963. |
| 10 | J. E. Rossiter and A. G. Kurn | Wind tunnel measurements of the unsteady pressures in and behind a bomb bay (Canberra).
A.R.C. C.P. 728. October, 1962. |
| 11 | G. B. Brown | The vortex motion causing edge tones.
<i>Proc. Phys. Soc.</i> , Vol. 49. 1937. |
| 12 | A. Powell | On the noise emanating from a two-dimensional jet above the critical pressure.
<i>Aero. Quarterly</i> , Vol. IV (II). February, 1953. |

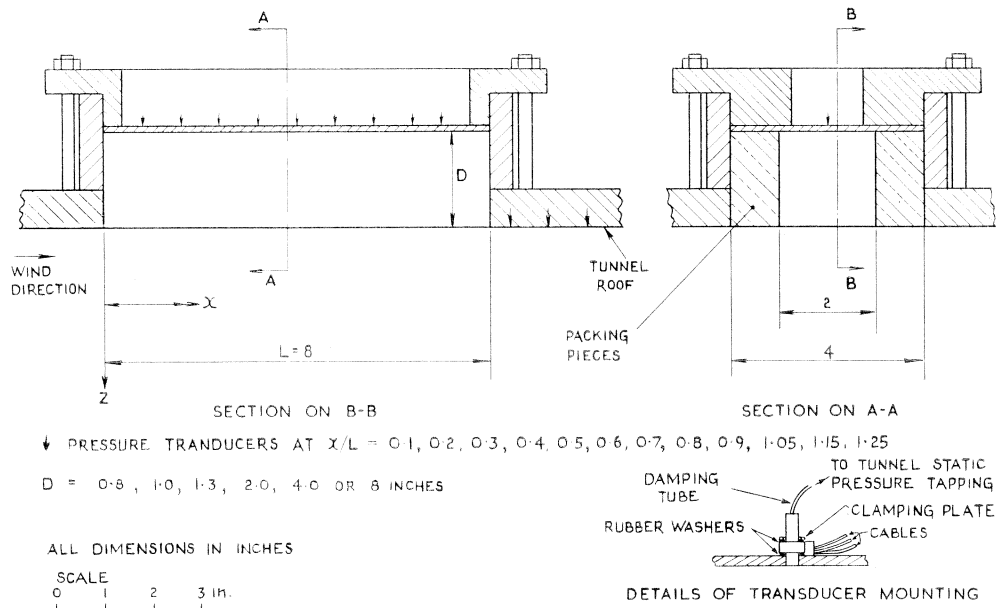


FIG. 1. General arrangement of cavities.

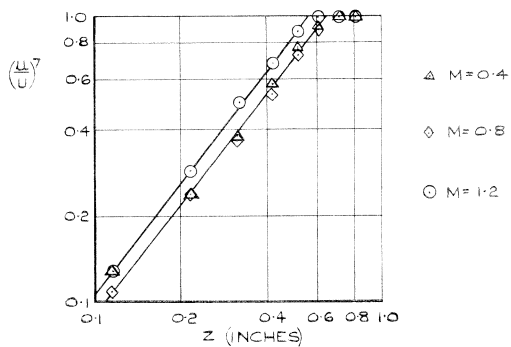


FIG. 2. Velocity profile of boundary layer on tunnel roof ($Re = 2 \times 10^6$ per foot).

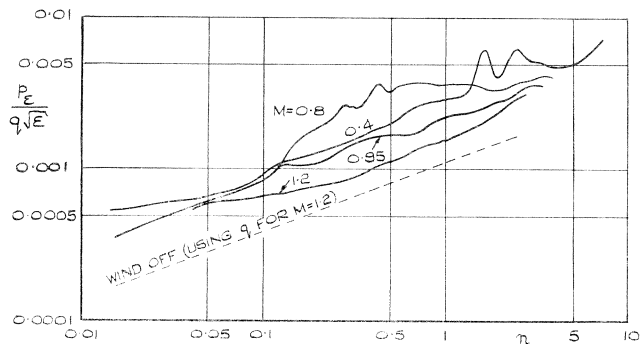


FIG. 3. Amplitude spectra of unsteady pressures on tunnel roof (no cavity) ($Re = 2 \times 10^6$ per foot).

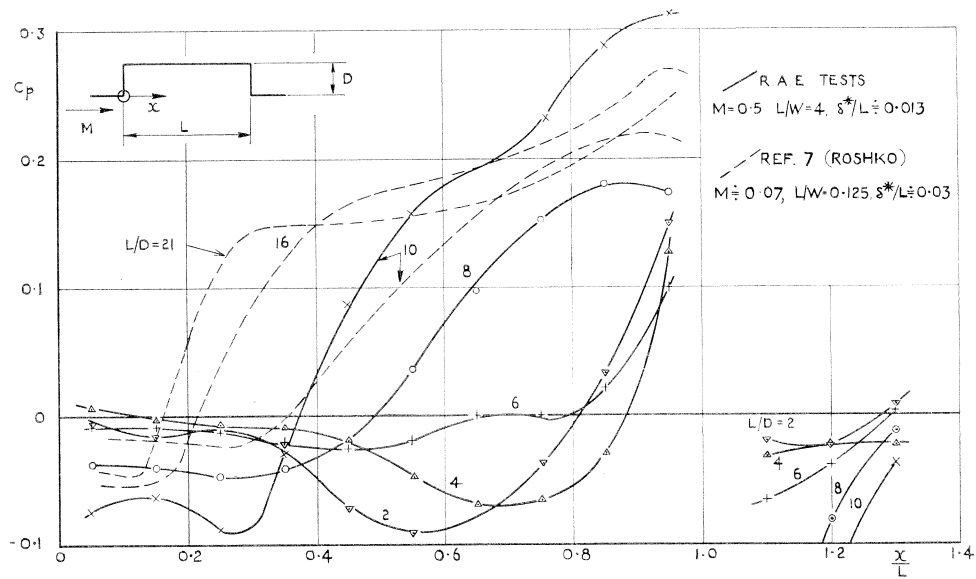


FIG. 4. Mean pressures on roof and behind cavities at low speed.

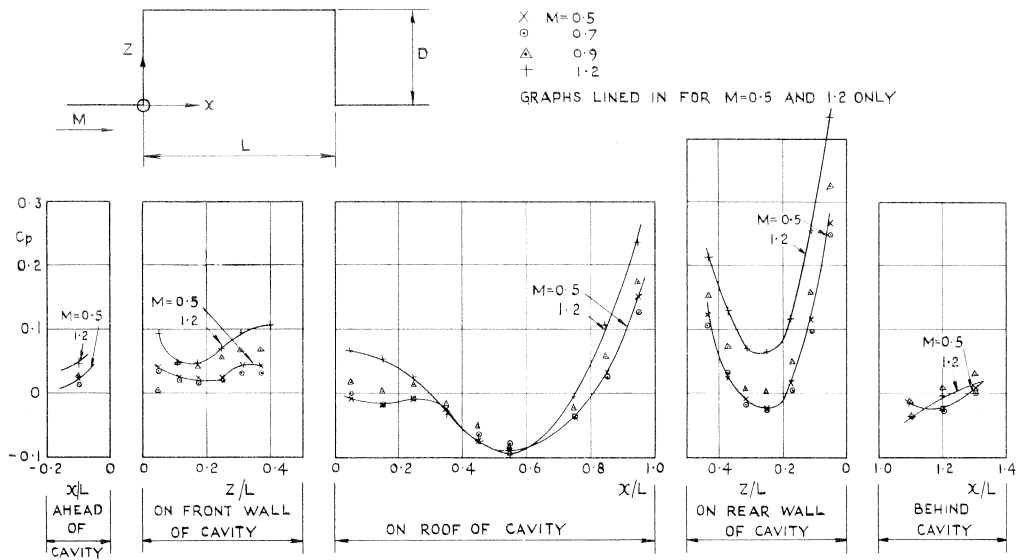


FIG. 5a. Effect of Mach number on mean pressures in and around cavity: $L/D = 4$.

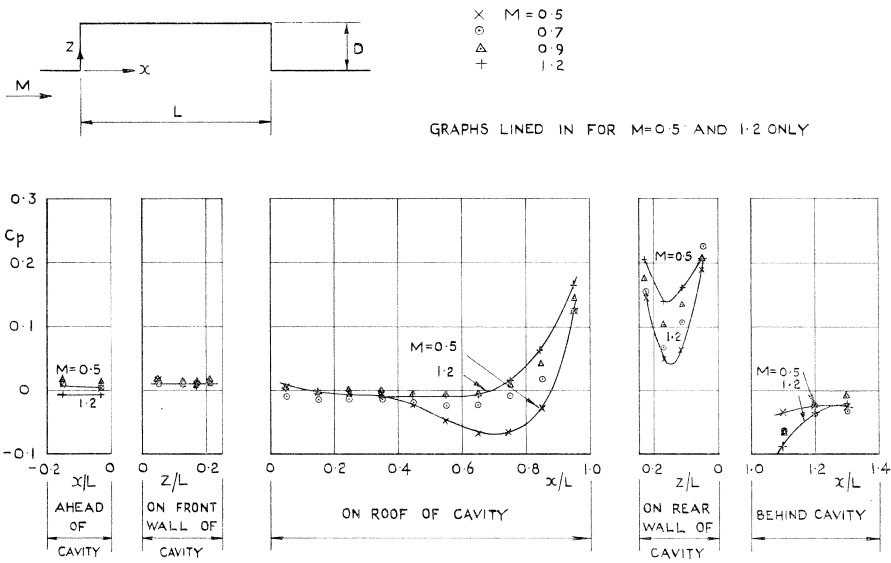


FIG. 5b. Effect of Mach number on mean pressures in and around cavity: $L/D = 4$.

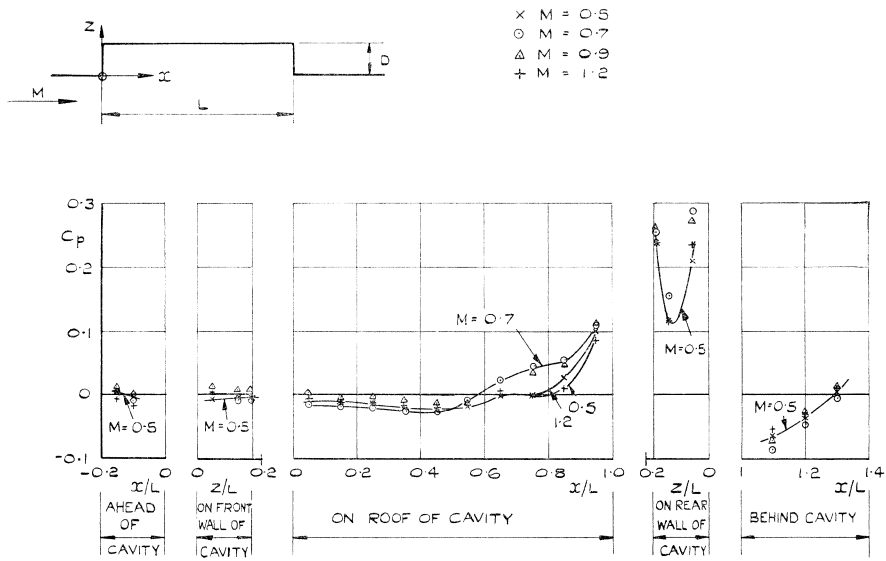


FIG. 5c. Effect of Mach number on mean pressures in and around cavity: $L/D = 6$.

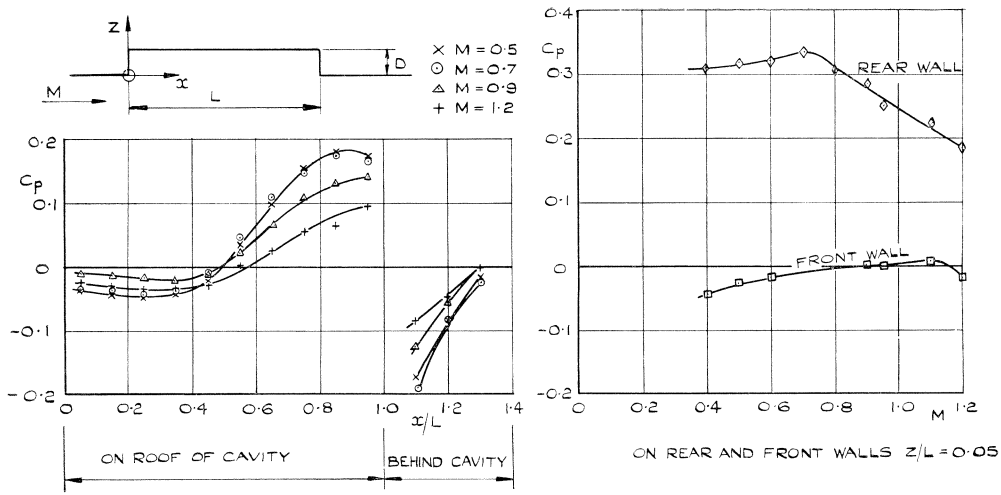


FIG. 5d. Effect of Mach number on mean pressures in and around cavity: $L/D = 8$.

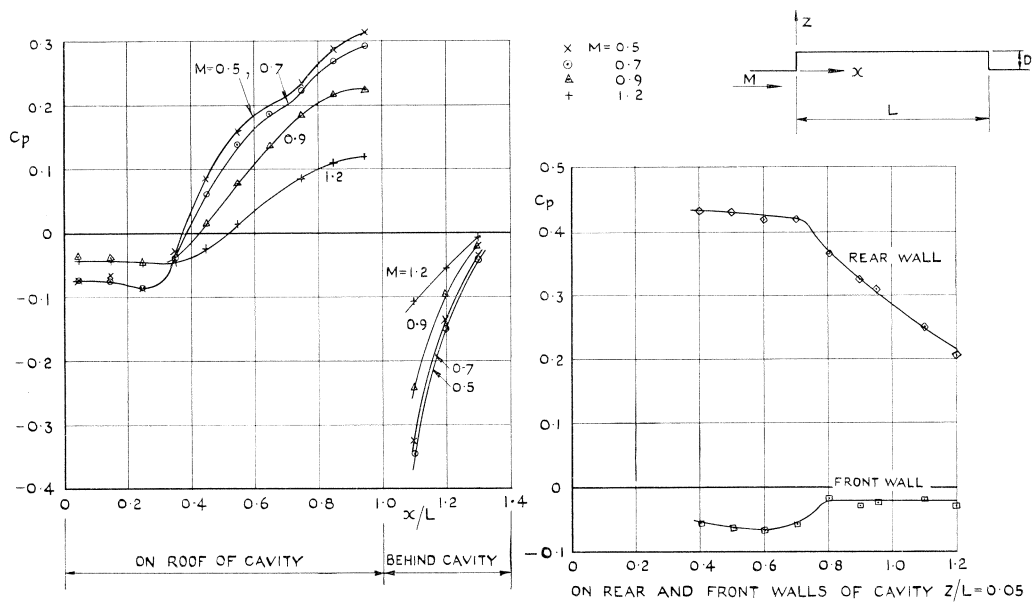
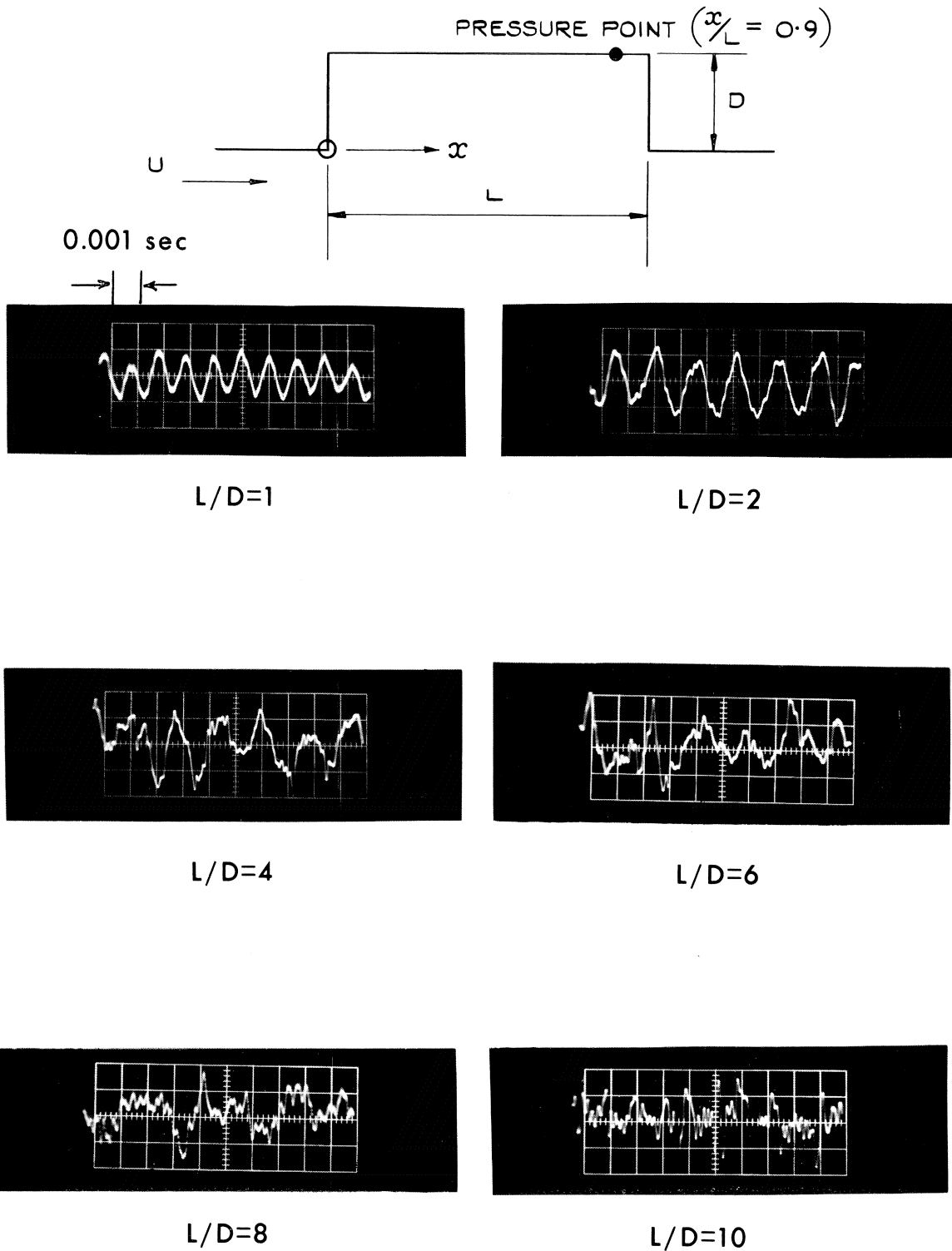


FIG. 5e. Effect of Mach number on mean pressures in and around cavity: $L/D = 10$.



(N.B. Arbitrary amplitude scales)

FIG. 6. Time histories of unsteady pressures in cavities: $M = 0.4$, $x/L = 0.9$.

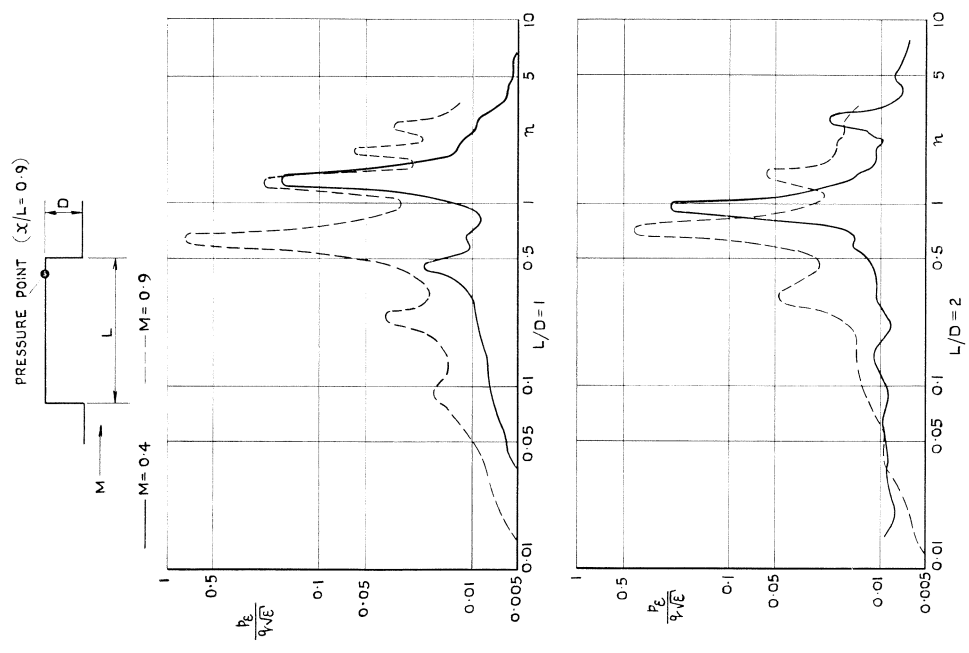
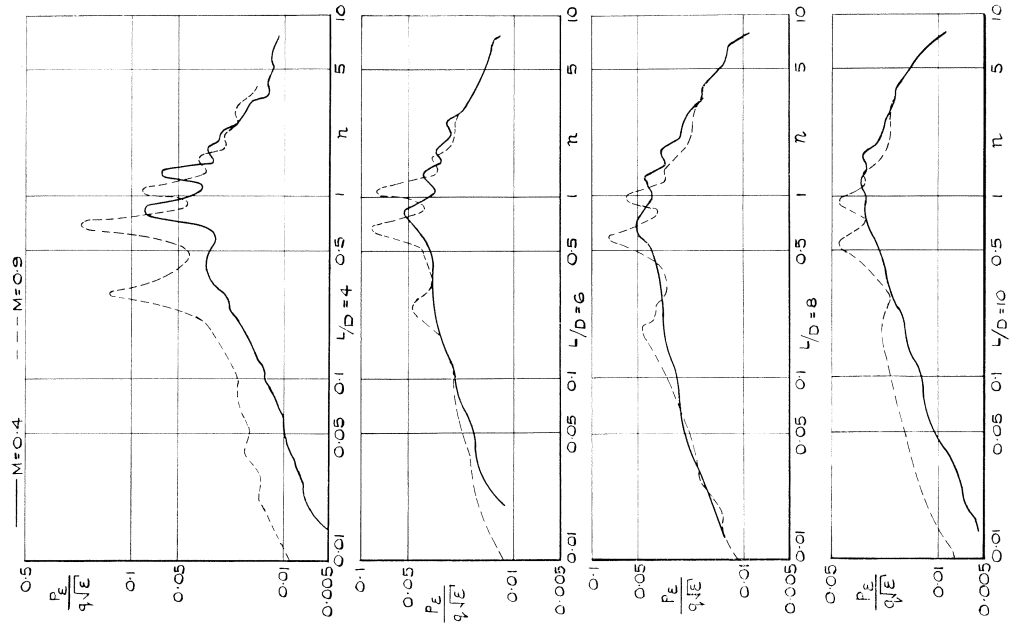


Fig. 7. Typical amplitude spectra of pressure fluctuations at rear of cavities: $x/L = 0.9$.

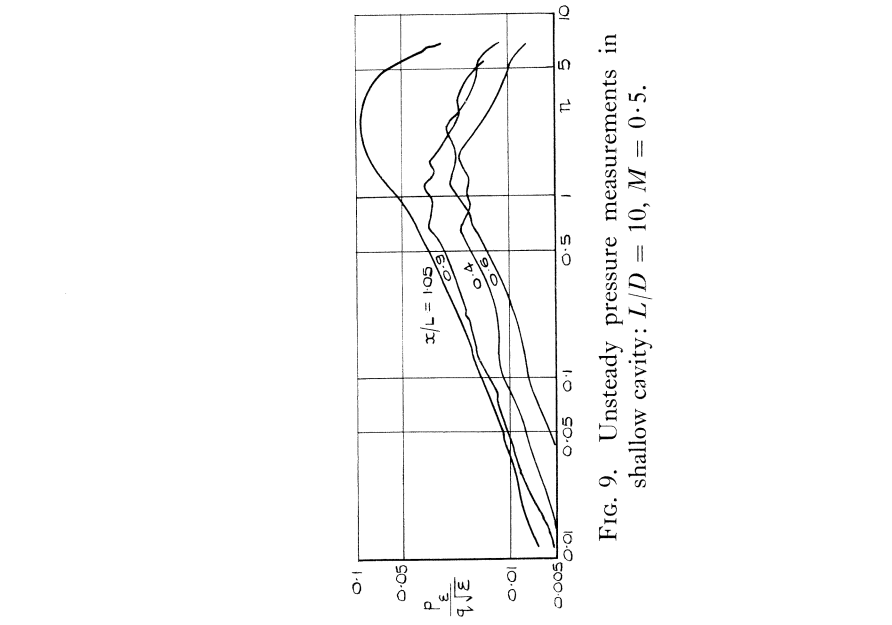


FIG. 8. Distribution of unsteady pressures in shallow cavities.

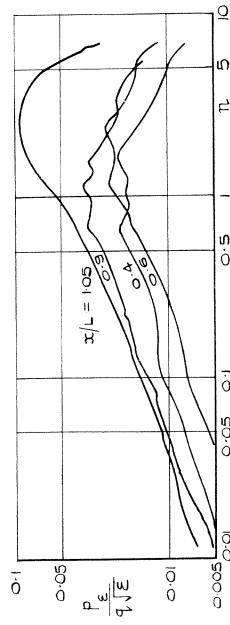


FIG. 9. Unsteady pressure measurements in shallow cavity: $L/D = 10$, $M = 0.5$.

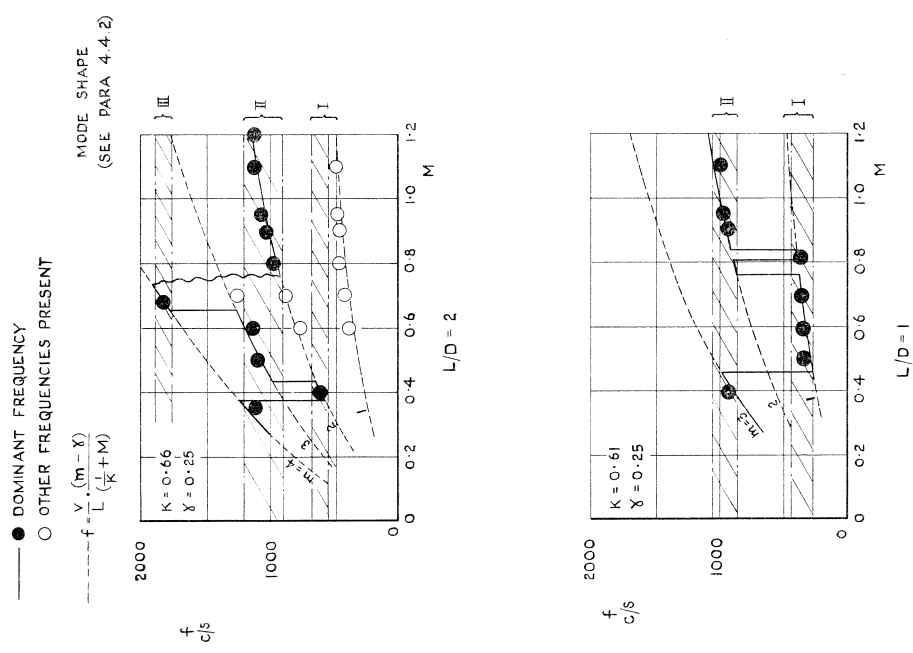


Fig. 10. Frequency of periodic pressure fluctuations in deep cavities.

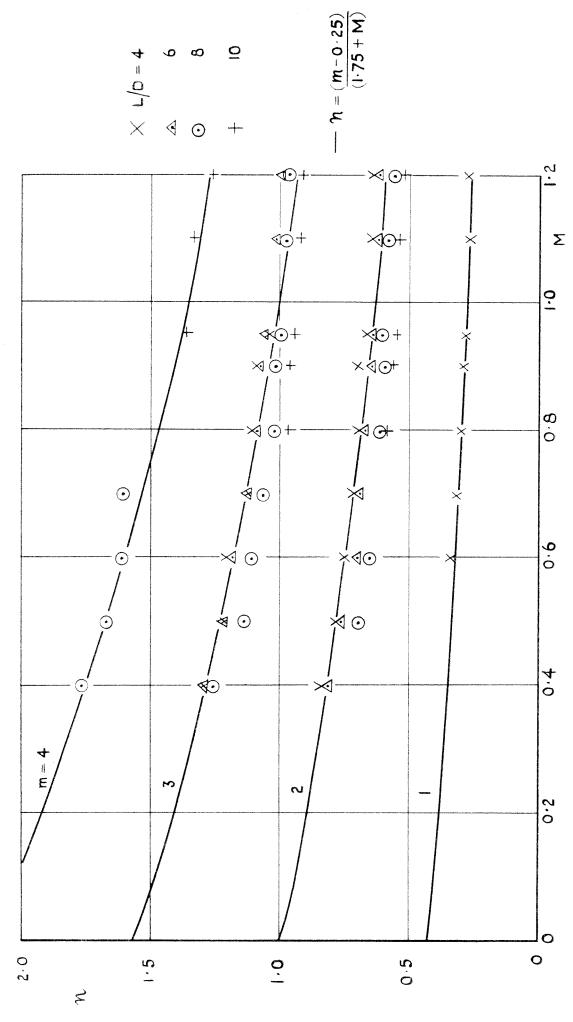


Fig. 11. Frequency of periodic pressure fluctuations in shallower cavities.

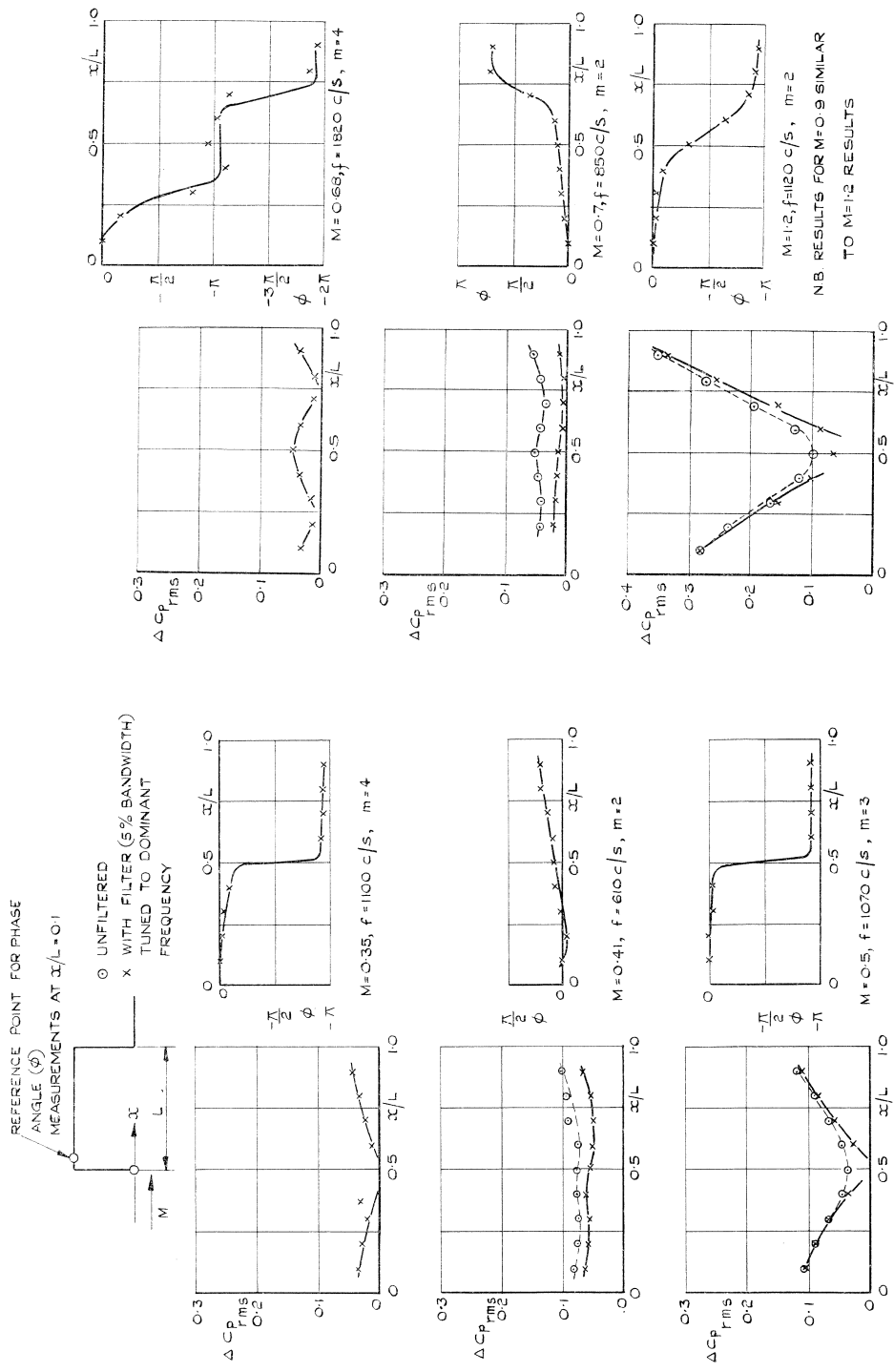


FIG. 12. Magnitude and phase of periodic pressure fluctuations in deep cavity: $L/D = 2$.

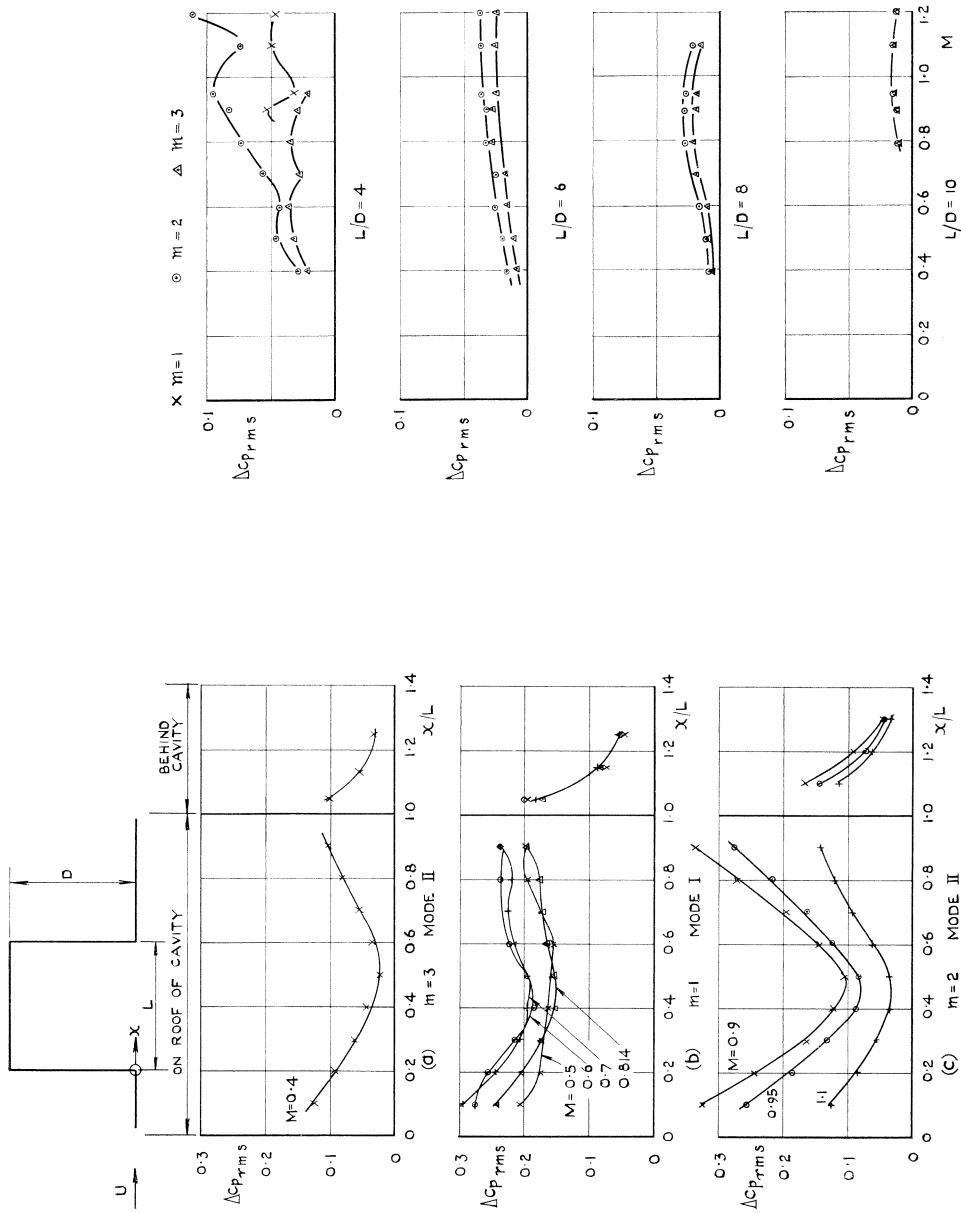


FIG. 13. Distribution of unsteady pressures in cavity with length/depth ratio = 1.

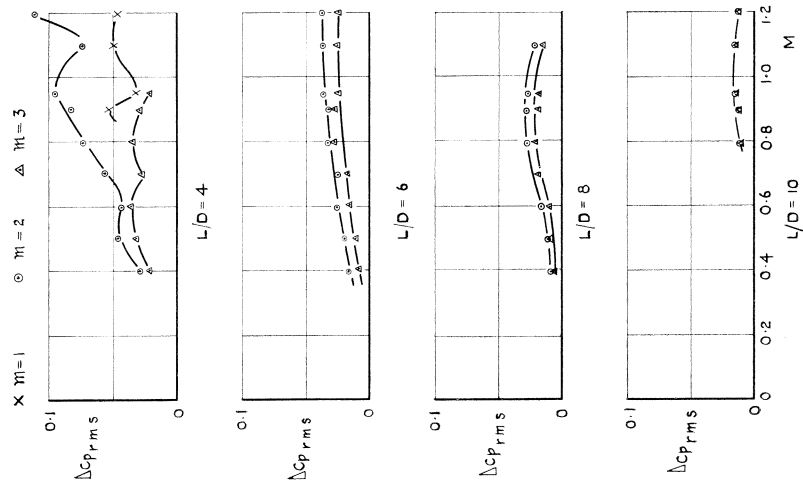


FIG. 14. Magnitude of periodic pressure fluctuations in medium and shallow cavities: $x/L = 0.9$.

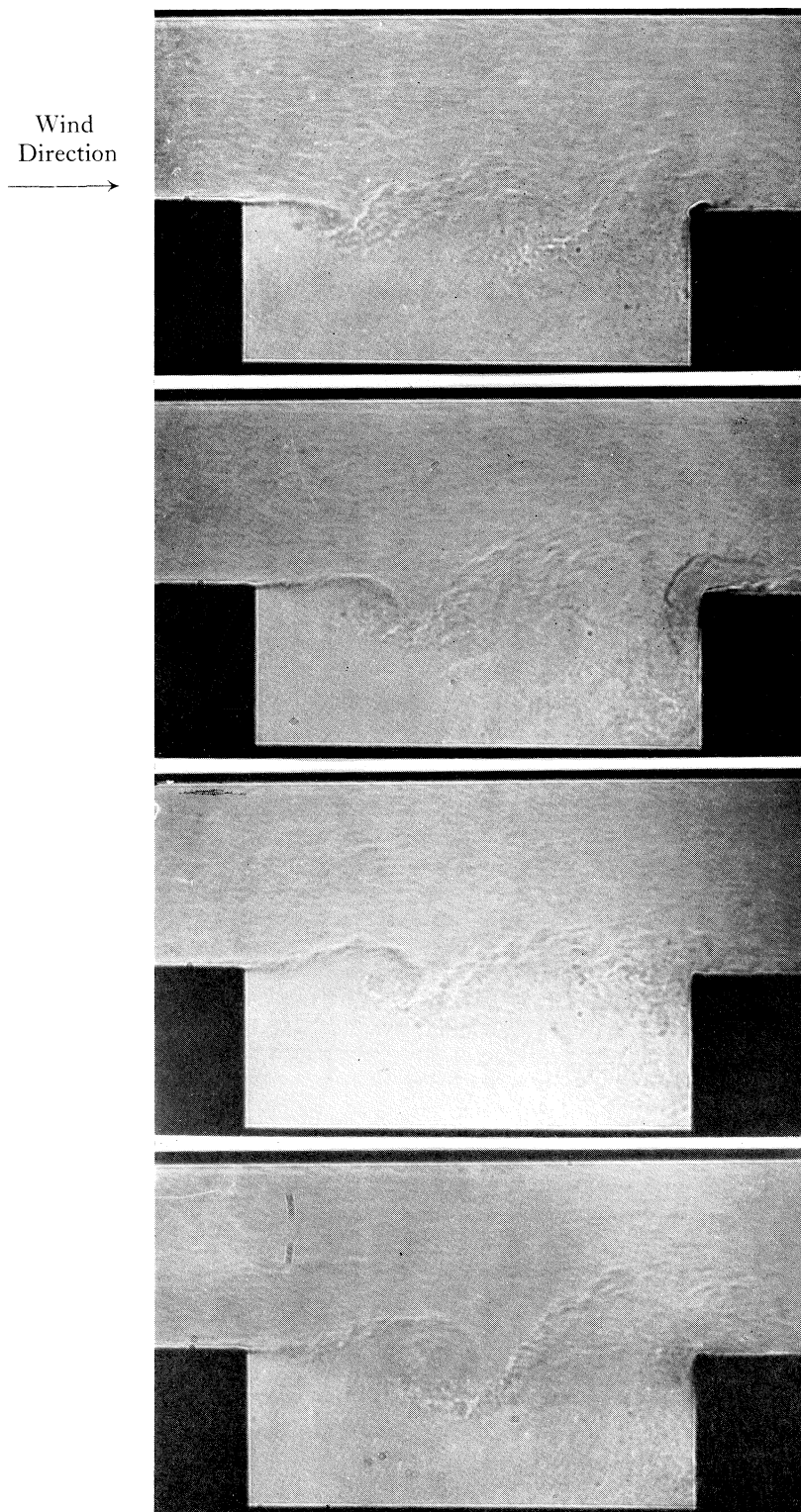
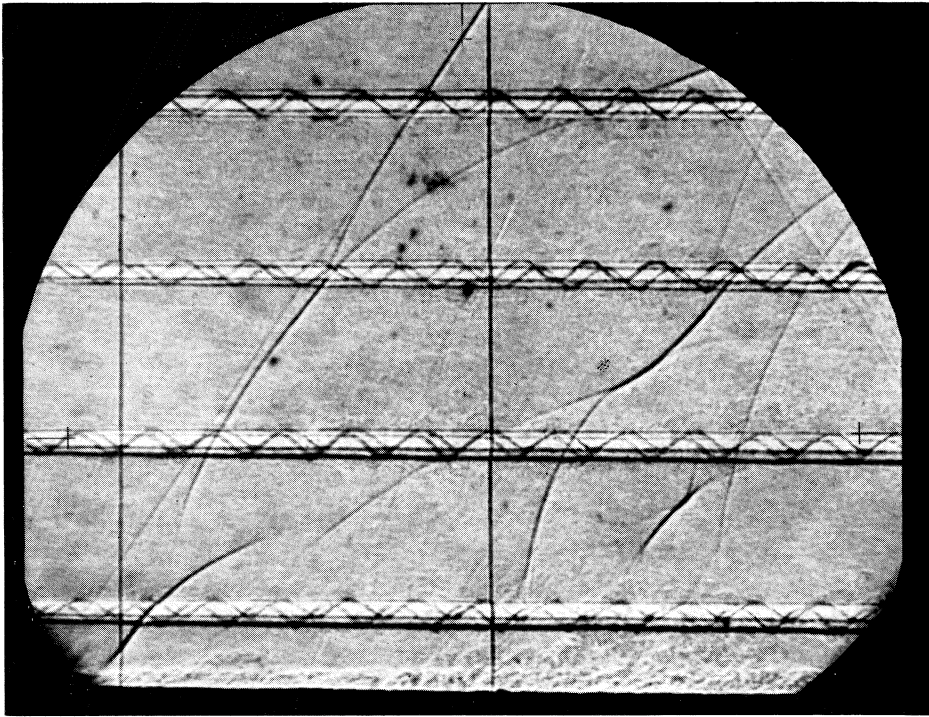
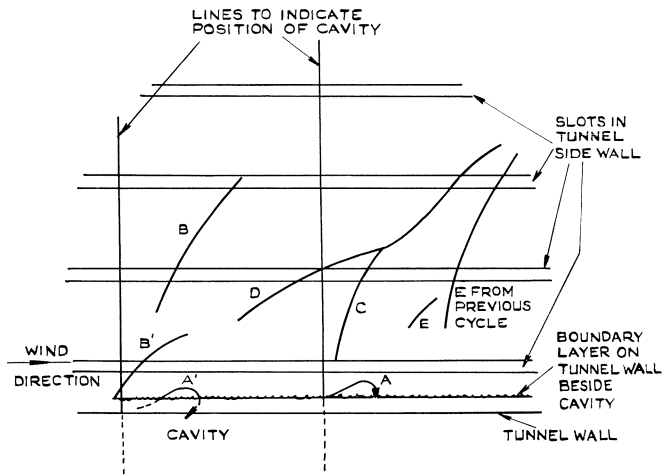


FIG. 15. Growth of vortex in shear layer: $M = 0.6$.
Two-dimensional cavity: $L/D = 4$ (laminar B.L.).

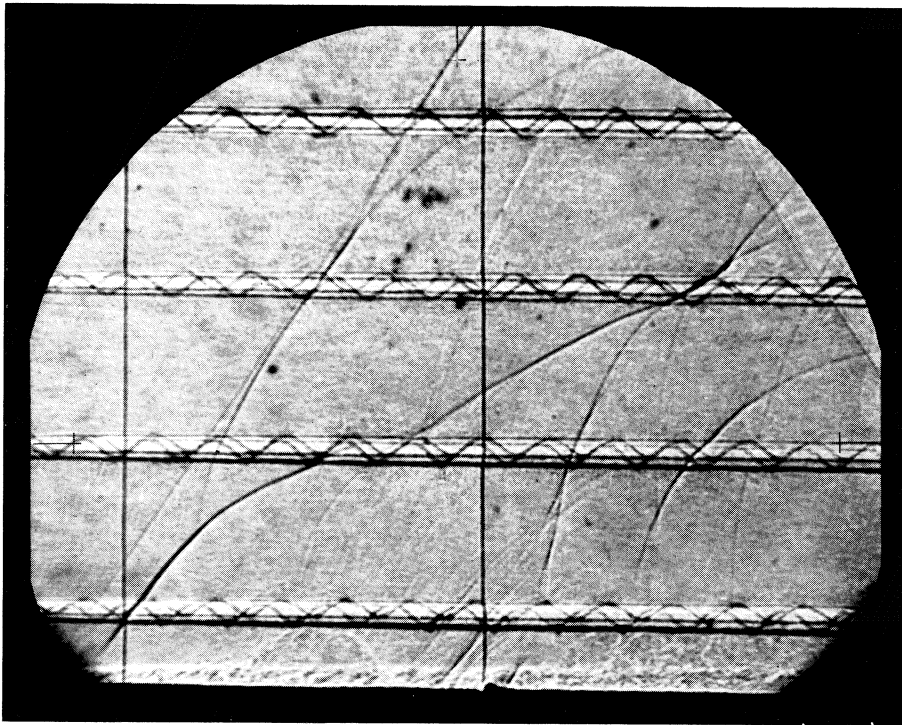


$t = 0.$

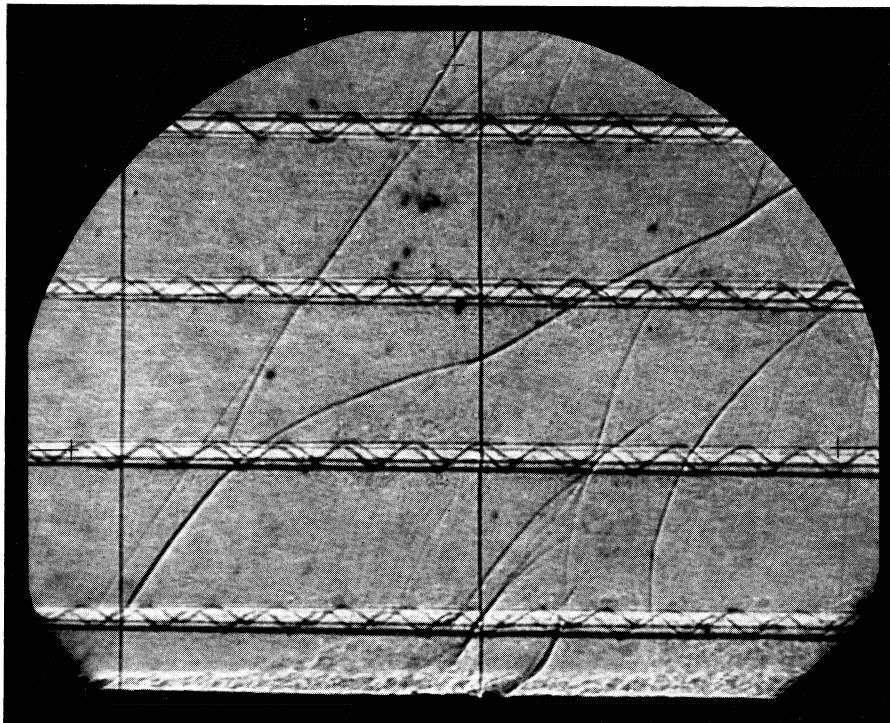


Interpretation of shadowgraph (see also Fig. 13).

FIG. 16. Shadowgraphs of the external flow over a resonating cavity:
 $M = 1.2, L/D = 2.$

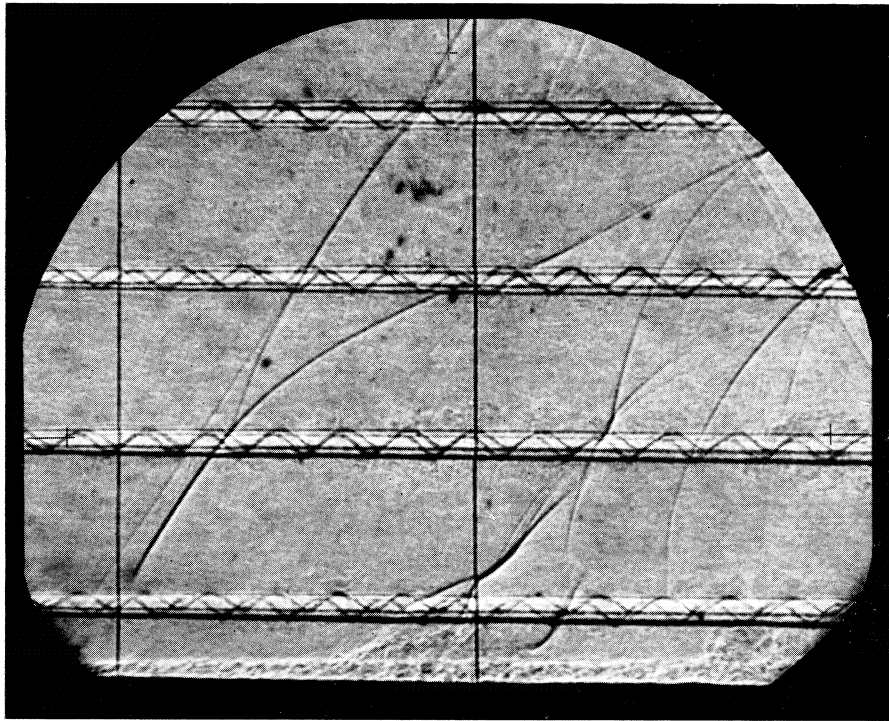


$t = 0.3T.$

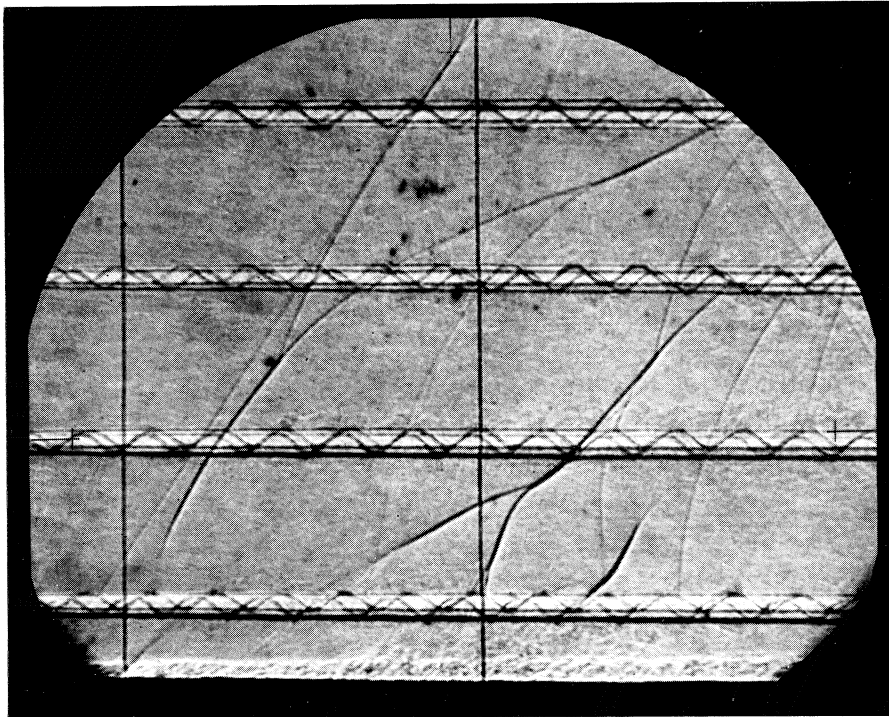


$t = 0.57T.$

FIG. 16—*continued.* Shadowgraphs of the external flow over a resonating cavity:
 $M = 1.2, L/D = 2.$



$t = 0.62T.$



$t = 0.77T.$

FIG. 16—concluded. Shadowgraphs of the external flow over a resonating cavity:
 $M = 1.2, L/D = 2.$

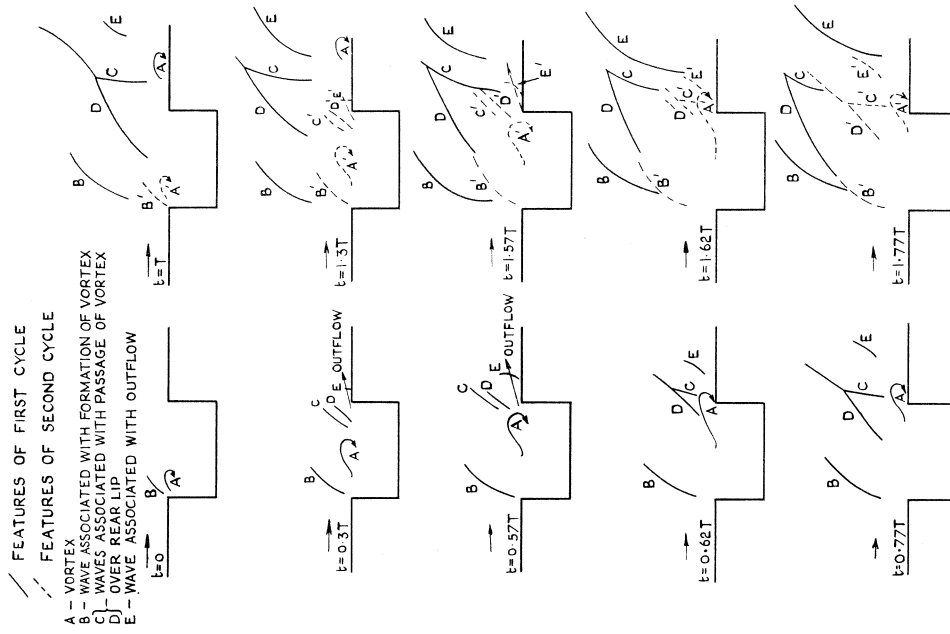


Fig. 17. The external flow over a resonating cavity $M = 1.2$, $L/D = 2$ (reconstructed from Fig. 16).

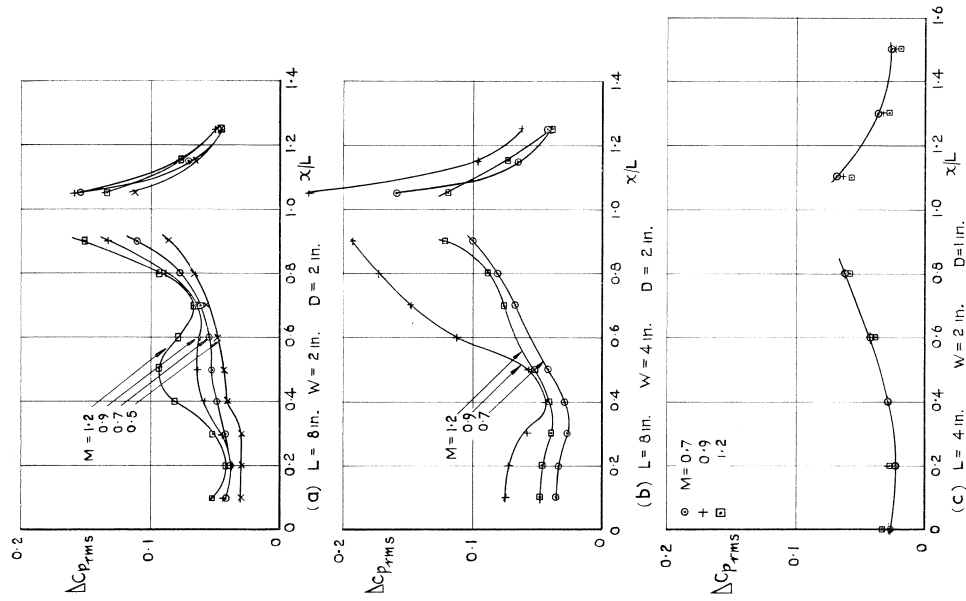


Fig. 18. Effect of cavity width and length on distribution of unsteady pressures: $L/D = 4$.

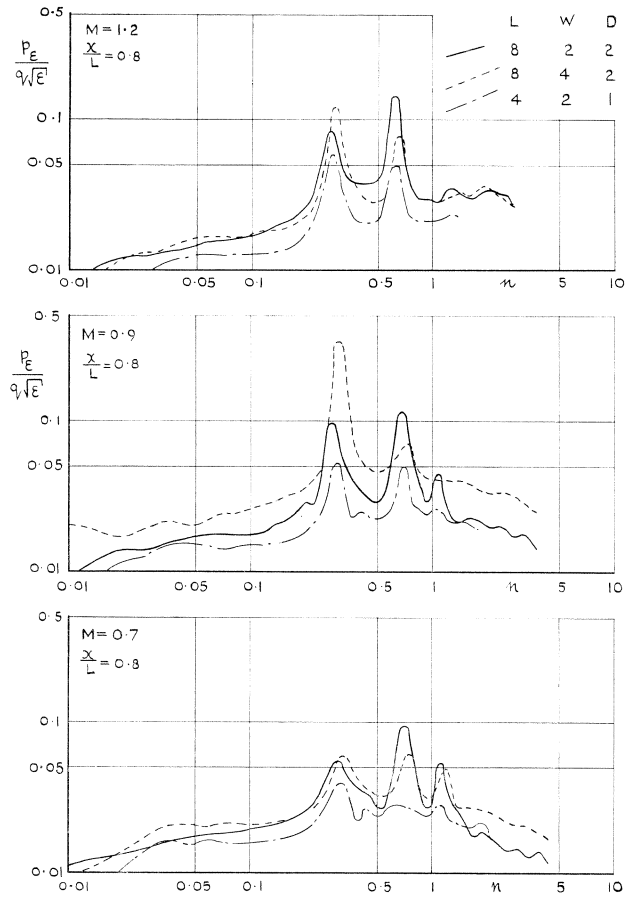


FIG. 19. Effect of cavity width and length on amplitude spectra of unsteady pressures: $L/D = 4$.

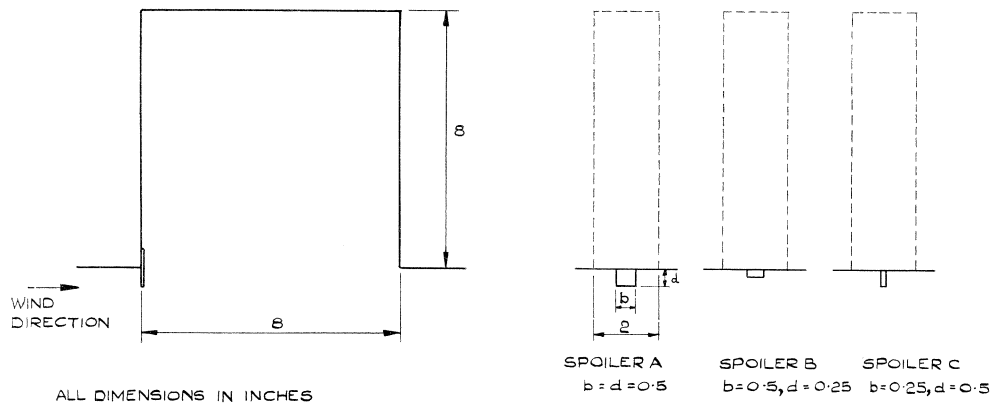


FIG. 20. Sketch of spoilers used with cavity with $L/D = 1$.

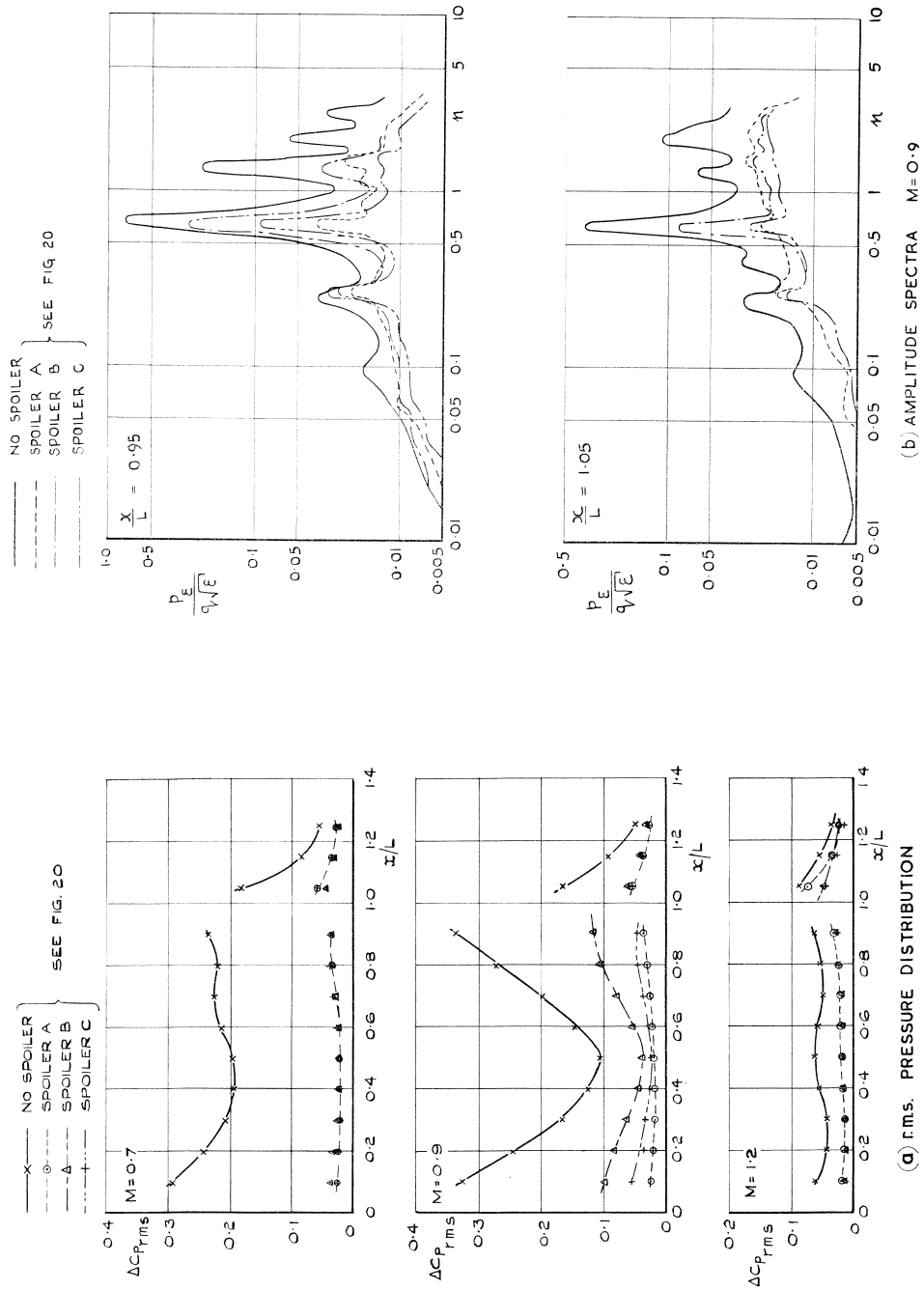


FIG. 21. Effect of spoilers on unsteady pressures: $L/D = 1$.

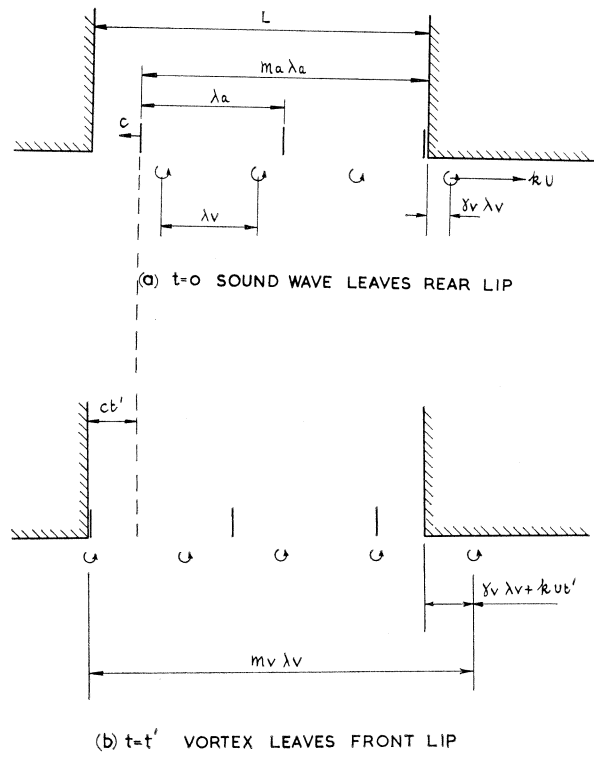


FIG. 22. Simplified model of flow over cavity.

<p>A.R.C. R. & M. 3438 October, 1964 J. E. Rossiter</p> <p>533.695.9: 533.6.048.2: 533.6.011.3</p> <p>WIND-TUNNEL EXPERIMENTS ON THE FLOW OVER RECTANGULAR CAVITIES AT SUBSONIC AND TRANSONIC SPEEDS</p> <p>Measurements have been made of the time average and unsteady pressures acting on the roof and behind a series of rectangular cavities set in the roof of the $2\text{ ft} \times 1\frac{1}{2}\text{ ft}$ transonic tunnel.</p> <p>It was found that the unsteady pressures contain both random and periodic components. The random component predominates in the shallower cavities (length/depth ratio > 4) and is most intense near the</p> <p>P.T.O.</p>	<p>A.R.C. R. & M. 3438 October, 1964 J. E. Rossiter</p> <p>533.695.9: 533.6.048.2: 533.6.011.3</p> <p>WIND-TUNNEL EXPERIMENTS ON THE FLOW OVER RECTANGULAR CAVITIES AT SUBSONIC AND TRANSONIC SPEEDS</p> <p>Measurements have been made of the time average and unsteady pressures acting on the roof and behind a series of rectangular cavities set in the roof of the $2\text{ ft} \times 1\frac{1}{2}\text{ ft}$ transonic tunnel.</p> <p>It was found that the unsteady pressures contain both random and periodic components. The random component predominates in the shallower cavities (length/depth ratio > 4) and is most intense near the</p> <p>P.T.O.</p>
<p>A.R.C. R. & M. 3438 October, 1964 J. E. Rossiter</p> <p>533.695.9: 533.6.048.2: 533.6.011.3</p> <p>WIND-TUNNEL EXPERIMENTS ON THE FLOW OVER RECTANGULAR CAVITIES AT SUBSONIC AND TRANSONIC SPEEDS</p> <p>Measurements have been made of the time average and unsteady pressures acting on the roof and behind a series of rectangular cavities set in the roof of the $2\text{ ft} \times 1\frac{1}{2}\text{ ft}$ transonic tunnel.</p> <p>It was found that the unsteady pressures contain both random and periodic components. The random component predominates in the shallower cavities (length/depth ratio > 4) and is most intense near the</p> <p>P.T.O.</p>	<p>A.R.C. R. & M. 3438 October, 1964 J. E. Rossiter</p> <p>533.695.9: 533.6.048.2: 533.6.011.3</p> <p>WIND-TUNNEL EXPERIMENTS ON THE FLOW OVER RECTANGULAR CAVITIES AT SUBSONIC AND TRANSONIC SPEEDS</p> <p>Measurements have been made of the time average and unsteady pressures acting on the roof and behind a series of rectangular cavities set in the roof of the $2\text{ ft} \times 1\frac{1}{2}\text{ ft}$ transonic tunnel.</p> <p>It was found that the unsteady pressures contain both random and periodic components. The random component predominates in the shallower cavities (length/depth ratio > 4) and is most intense near the</p> <p>P.T.O.</p>

rear wall. The periodic component predominates in the deeper cavities (length/depth ratio < 4) and may form standing wave patterns. It is suggested that the periodic component is due to an acoustic resonance within the cavity excited by a phenomenon similar to that causing edge-tones. It may be suppressed by fixing a small spoiler at the front of the cavity.

rear wall. The periodic component predominates in the deeper cavities (length/depth ratio < 4) and may form standing wave patterns. It is suggested that the periodic component is due to an acoustic resonance within the cavity excited by a phenomenon similar to that causing edge-tones. It may be suppressed by fixing a small spoiler at the front of the cavity.

rear wall. The periodic component predominates in the deeper cavities (length/depth ratio < 4) and may form standing wave patterns. It is suggested that the periodic component is due to an acoustic resonance within the cavity excited by a phenomenon similar to that causing edge-tones. It may be suppressed by fixing a small spoiler at the front of the cavity.

rear wall. The periodic component predominates in the deeper cavities (length/depth ratio < 4) and may form standing wave patterns. It is suggested that the periodic component is due to an acoustic resonance within the cavity excited by a phenomenon similar to that causing edge-tones. It may be suppressed by fixing a small spoiler at the front of the cavity.

© *Crown Copyright 1966*

Printed and published by
HER MAJESTY'S STATIONERY OFFICE

To be purchased from
49 High Holborn, London WC1
423 Oxford Street, London W1
13A Castle Street, Edinburgh 2
109 St. Mary Street, Cardiff
Brazennose Street, Manchester 2
50 Fairfax Street, Bristol 1
35 Smallbrook, Ringway, Birmingham 5
80 Chichester Street, Belfast 1
or through any bookseller

Printed in England